Heliyon 8 (2022) e10824

Contents lists available at ScienceDirect

Heliyon

journal homepage: www.cell.com/heliyon

Research article

Design and experimental evaluation of a Venturi and Venturi-Vortex microbubble aeration system

Esteban De Oro Ochoa [a], Mauricio Carmona García [a,*], Néstor Durango Padilla [a], Andrés Martínez Remolina [b]

[a] Mechanical Engineering Department, Universidad del Norte, Barranquilla, Colombia
[b] Association for the Development of Aquaponics in Colombia "ADACOL", Colombia

ARTICLE INFO

Keywords:
Micro-nano bubbles
Experimental evaluation
Aeration efficiency
Oxygen transfer rate
Venturi
Venturi-vortex

ABSTRACT

This work presents an experimental evaluation of a Venturi and Venturi-Vortex microbubble aeration system, taking as input variables the water-air flow ratio, water renewal time and area-volume ratio of the water tank. The aeration process response variables are defined in terms of oxygen transfer and aeration efficiency through the standard volumetric mass transfer coefficient (K_La_{20}), standard oxygen transfer rate (SOTR), and standard aeration efficiency (SAE). Two methods of air injection were analyzed: 1. Air injection in the throat chamber of the Venturi generator; 2. air supplying in the suction side of the hydraulic pump of the aeration system. Experimental results indicate that the water renewal time variable (RT) is a statistically significant factor with respect to the K_La_{20}, which can be maximized by decreasing RT. The effects of the variable flow ratio (FR) are greater than the effects of renewal time and area-volume ratio (AVR) concerning SOTR and SAE, indicating a maximum response with a minimum flow ratio, using the Venturi-Vortex microbubble generator. When the flow ratio decreases, the air flow increases, generating and transferring a greater amount of microbubbles (MB) into the water. It was found that increasing the air flow produced an increase in the standard oxygen transfer rate SOTR and standard aeration efficiency SAE. Results allow concluding that the injection of the air flow from the suction side of the pump promotes the generation of microbubbles (MB) for a maximum air flow allowed by the system. SOTR and SAE could be maximized whit the flow ratio factor and the Venturi-Vortex generator, supplying air flow from the suction side of the hydraulic pump.

1. Introduction

Aeration systems are essential in semi-intensive and intensive aquaculture to maintain an environment consistent with the physiological requirements of the cultured organisms, in order to diffuse air particles that allow oxygen to be transferred to the water [1]. Aeration provides oxygen to bacteria for wastewater treatment and keeps aquatic plants and animals alive while they consume dissolved oxygen (DO) from the water. The most commonly used aeration systems in aquaculture are gravity, surface, diffuser and turbine aerators, spiral aerators, propeller vacuum pump aerators, stepped cascade aerators including circular stepped waterfall aerators, clustered circular stepped waterfall aerators and some other types [2]. However, the bubbles generated by these devices are millimeter-sized and have a faster ascent rate in the water than a micro bubble [3].

Microbubble aeration systems have been investigated and developed to improve the oxygen transfer, the separation of particles from the water and the reproductive conditions of aquatic animals and microorganisms. A summary of the direct background to this work is presented below.

Huang et al. [4] revised experimental and theoretical works about parameters that influence the bubble rupture and the performance of Venturi-type bubble generators. They conclude that the performance of the Venturi-type bubble generator mainly depends on the flow conditions (gas and liquid) and the geometric configuration. In addition, the rapid deceleration of the bubble, the dramatic expansion and contraction in the divergent zone of the Venturi generator have significant effects on the final rupture of the bubble. Yadav et al. [5] studied the geometric parameters of a Venturi tube, e.g. the throat length, number of air holes and convergent and divergent angles, in order to optimize the device and achieve the highest aeration efficiency. Authors found an optimal

* Corresponding author.
E-mail address: mycarmona@uninorte.edu.co (M. Carmona García).

https://doi.org/10.1016/j.heliyon.2022.e10824
Received 13 July 2022; Received in revised form 5 September 2022; Accepted 26 September 2022

performance with a throat length of 100 mm, 17 air inlet holes, converging and diverging angles of 15°, achieving a maximum standard oxygen transfer rate (SOTR) and standard aeration efficiency (SAE) of 0.0216 kgO_2/h and 0.611 kg O_2/kWh, respectively. Concerning micro and nano bubble generator designs, authors as Zhao et al. [6] studied the individual movement of fine bubbles using a Venturi-type generator. A rapid deceleration of the bubbles in the divergent zone of the Venturi tube triggers a process of rupture in very tiny bubbles, and the increase of the liquid flow rate could intensify the collapse process. Lee et al. [7] studied the variation of the inlet and exit angles of the Venturi nozzles on the formation of micro bubbles. The main founding of the authors include that the pressure drop depends on the exit angle, the air flow rate did not vary linearly with the water flow and bubbles collapse at the beginning of the divergent angle of the Venturi generator was observed. Li et al. [8] investigated numerically and experimentally the influence of different geometric parameters on the onset of cavitation. They found that the onset of cavitation was determined by flow resistance, which is significantly dependent on the geometric design of the Venturi tube. Additionally, a small draft angle results in low cavitation onset and high microbubble production. In order to evaluate the mean size and volume of pico and nano bubbles, Yu & Felicia [9] conducted an experimental design to investigate the effects of the ratios of inlet and throat diameter, throat diameter-length, and inlet and exit angles in Venturi tubes. Michailidi et al. [10] designed a rotating flow type nano bubble generator, they evaluated the behavior of the nanobubbles (NB) taking into account the hydrodynamic diameter and the electrical potential as a function of processing time, gas type, pH value of water and NaCl concentration. According to the results, the mechanism of generation of bulk NB and its long-term stability mainly can be attributed to the interactions of hydrogen bonds, which promote the formation of a stable interface layer, with nanobubbles within the water for up to three months. Suwartha et al. [3] evaluated the results of the volumetric mass transfer coefficients in a conventional Venturi-type micro bubble generator (MBG), a Venturi with internal sphere of cavitant surface and a vortex-type generator. They measured the contact time of the MB in the water generated by each device. Results showed that the smallest bubble size was produced by the MBG vortex type with an average bubble diameter of 89 μm and the slowest ascent rate of 17.67 m/h. It also produced the highest K_La of 0.297 min^{-1}, with an aeration contact time of 3.64 min. Wang et al. [11] presented a comparison between a Venturi MBG and a Swirl-Venturi MBG with tangential inputs, observing the single bubble rupture phenomena. Three different rupture patterns were observed (i.e. tensile rupture, dynamic erosive rupture, and static erosive rupture) in the Swirl-Venturi MBG, whereas in the Venturi MBG there was only a tensile rupture. Using a high-speed photography and the DO concentration measured, Wang et al. [12] evaluated the liquid volumetric mass transfer coefficient (K_La) in a Venturi and a Swirl-Venturi MBG. The Swirl-Venturi MBG produces more microbubbles with a smaller Sauter mean diameter than the Venturi MBG. In addition, the K_La of the Swirl-Venturi MBG was higher than that of the Venturi MBG at high surface gas velocity, and the maximum stable bubble size of the Swirl-Venturi MBG is also smaller than that of the Venturi MBG.

Previous works have shown the advantages of NB and MB in different areas, including aeration, most of these works have focused on the study of the average size and volume of bubbles, generated in devices with particular designs working under the Venturi principle and rotary flow. MB and NB have desirable abilities to acquire free radicals, which allows the degradation of toxic compounds, water disinfection, cleaning/descaling of solid surfaces and promotes the physical-chemical conditions to dissolve oxygen in water [13]. Nevertheless, the application of NB to improve the water quality is not adequate due to the low sediment separation efficiency, the NB can contain solid particles and hold them in suspension for long times [14]. Since the residence time of MB is lower than that of NB, the application of MB mitigates this problem. According to Agarwal et al. [13], it is possible to generate a high-density of MB with a diameter lower than 100 microns using a Venturi-type MBG, which has a compact size and can be operated with low pumping power. NB generators have higher acquisition and operational costs due to the construction materials used and the operational pressure required. In this sense, Favvas et al. [15] indicate that NB can be generated by the membrane method, which injects a high-pressure gas through a porous material and creates a cloud of bubbles and NB of different sizes. NB can also be generated with the injection of a mixture of gas and water through a porous membrane, however, these devices require a high pumping capacity and operating pressure. A different method for the NB generation is the use of an ultrasonic palladium electrode, which produces a mean bubble diameter from 300 to 500 nm [16]. NB have longer residence times in water than MB, which is an innate advantage in these applications. However, compared to MB systems, NB production requires more complex systems, higher energy requirements, higher operating costs, and the longer residence times can be a disadvantage in many applications for the solid suspension. On the other hand, large bubble systems are the cheaper systems, but have reduced capacity to mass transfer. Therefore, the production of MB is presented as a viable alternative in aeration systems, especially on a commercial scale.

Different works have introduced the good performance of Swirl-Venturi MBG. Nevertheless, there are no studies so far on MBG that analyze the factors of the water-air flow ratio, water renewal time, area-volume ratio of water and the simultaneous comparison of two microbubble generators operating under the Venturi and Venturi-Vortex effect. Besides, there are no previous studies that evaluated the micro bubble aeration systems based on aeration parameters such as the standard volumetric mass transfer coefficient (K_La_{20}), Standard Oxygen Transfer Rate (SOTR) and Standard Aeration Efficiency (SAE) simultaneously. Furthermore, Venturi generators are typically designed with an air injection chamber located in the throat of the device, but this can represent a limitation in conversion to MB from large bubbles. This research proposes the implementation of a MB aeration system, which allows the injection of air on the suction side of a regenerative pump. The combination of the air injection with the Vortex effect, has the potential to promote a higher conversion of MB, compared to a traditional Venturi generator. This kind of proposed system has not been analyzed so far.

This document as organized as follows. Section 2 presents the Venturi and Venturi-Vortex MBG characteristics and the experimental procedure, where a 2^{k-p} factorial design was carried out in order to evaluate the influence of the factors based on K_La_{20}, SOTR and SAE. Section 3 presents the statistical support of the collected data. Results and discussion are shown in section 4 and conclusions are presented in section 5.

2. Microbubble generator and experimental procedure

In this section, several design alternatives for Venturi microbubble generators and Vortex devices are considered. The qualitative MB production of the generators is compared individually. Two alternatives are shown for the air injection in the Venturi and Venturi-Vortex generator. To distinguish the devices with the better generation of microbubbles, a comparative analysis was carried out by qualitative visualization. In this section, the design of the experimental platform of the MB aeration system, the experimental factors, response variables and the procedure for data collection are described.

2.1. Microbubble generators

Following the geometric characteristics recommended by Li et al. [8] and Yu & Felicia [9] a Venturi and a Venturi-Vortex MBG were fabricated. The general dimensions of the Venturi generator and vortex devices are presented in Annex 1 (a) of the supplementary material. Annex 1 (b) and (c) shows the design and dimensions of two Vortex devices, one of them with a cylindrical geometry and the another one with finned surfaces. Device in Annex 1 (b) produces a swirl of the water-air mixture in the internal structure of the cylinder. Device presented in Annex 1 (c) can be installed inside the pipe and it is located before the convergent

zone of the Venturi generator. The main objective of the Vortex devices is to combine the Venturi cavitation effect with the swirl to generate a greater quantity of MB by breaking-up.

2.2. Comparative analysis of microbubble generators

In order to maximize the generation of air MB and select the best alternatives, preliminary tests of different configurations were carried out to observe the general performance and the production of MB. One way to verify the presence of MB is to observe the cloudy appearance in the water with white color (also known as white water). Figure 1 shows the presence of MB in a water sample at three different times. In the beginning, the presence of many MB can be observed throughout the water column, after 40 s the water acquires a transparent appearance in the lower section of the container, the MB leave the water towards the atmosphere through the upper section, after 80 s most of the air particles have been displaced by the effect of buoyancy. The behavior of the air microbubbles obeys a Brownian movement and their prolonged presence will allow a uniform transference of oxygen in the water column. The oxygen transfer process depends directly on the gas and liquid phases contact. In addition, the generation of MB with a pumping system will facilitate the recirculation of the water and the constant accumulation of MB in the liquid phase, which could increase the rate of oxygen transfer.

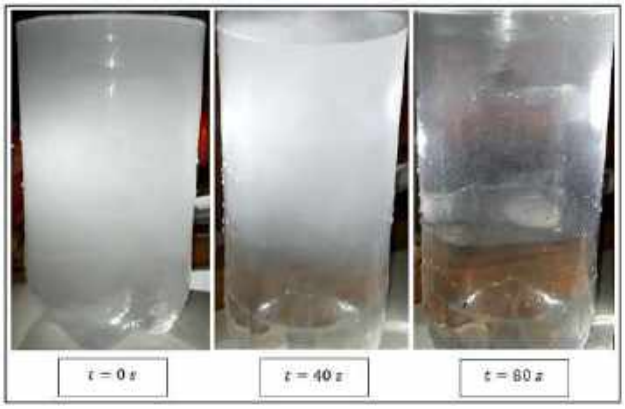

Figure 1. Qualitative presence of microbubbles in the water for different times.

Figure 2 (a) (b) and (c) shows a qualitative comparison of microbubbles generated with different combination of Venturi MBG with Vortex devices, using different air intake methods operating under the same water and air flow conditions. Figure 2 (a) shows the Venturi-Vortex MBG with an air injection chamber of 1.5 mm internal diameter, which is located in the throat section of the device. Figure 2 (b) and (c) shows the Venturi-Vortex MBG without air injection chamber, in this case, the air inlet is carried out on the suction side of the pump of the aeration system.

Qualitatively, the Venturi-Vortex MBG presented in Figure 2 (b) shows a higher generation of MB compared to the other designs. The Venturi-Vortex configuration of Figure 2 (a) shows a lower production of MB compared with the Venturi-Vortex design of Figure 2 (c). However, in the device of Figure 2 (c) a reduction of the water flow of 55% compared to the designs in Figure 2 (a) and (b) is obtained.

Preliminary results allow to distinguish a higher generation of MB in the Venturi-Vortex hybrid device presented in Figure 2 (b). The swirl effect of this device is generated from the suction line of the pump, this effect is imparted to both the water and the air phases and helps in the shearing that promotes the generation of MB. This effect may be undone in the injection chamber of devices such as the one shown in Figure 2 (a). Considering the formation of MB and the operational conditions, two modes of operation with the Venturi and Venturi-Vortex generator design will be analyzed to make comparisons in terms of oxygen transfer rate and aeration efficiency. Due to the selected Venturi generator does not have an air injection chamber, the air supply is accomplished in the suction line of the hydraulic pump.

2.3. Experimental platform

Figure 3 shows the developed experimental platform, which includes the MB aeration system. In general, this system is composed by a hydraulic pump, a Venturi tube on the suction side of the pump to mix the liquid and gas phase, a Venturi or Venturi-Vortex microbubble generator, and a pressure gauge located on the discharge side of the pump.

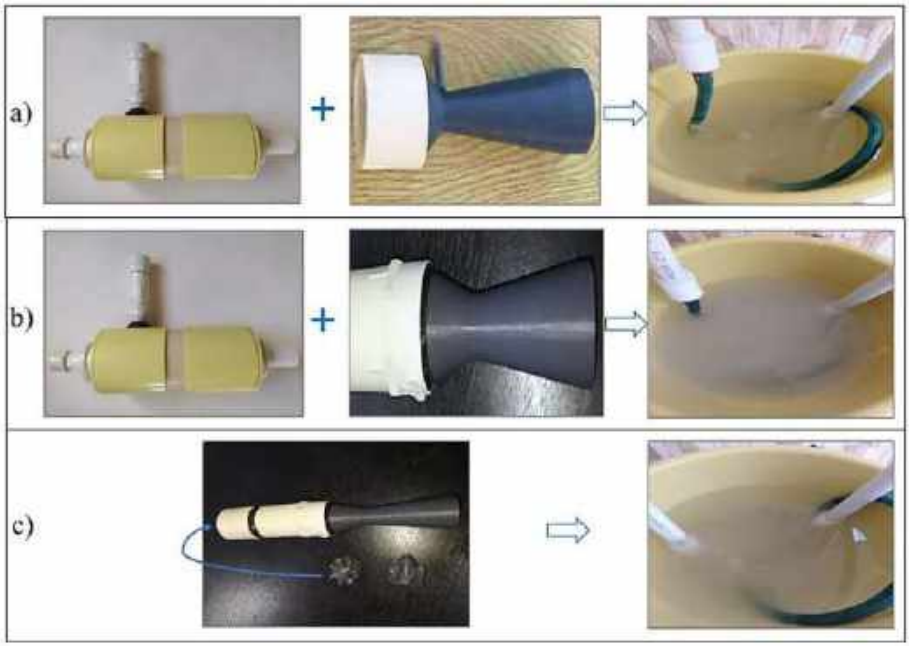

Figure 2. Vortex device designs. (a) Venturi-Vortex with φ 1.5 mm air injection chamber; (b) Venturi-Vortex without air injection chamber (air injection from the suction side of a pump); (c) Venturi-Vortex with finned surfaces and without air injection chamber.

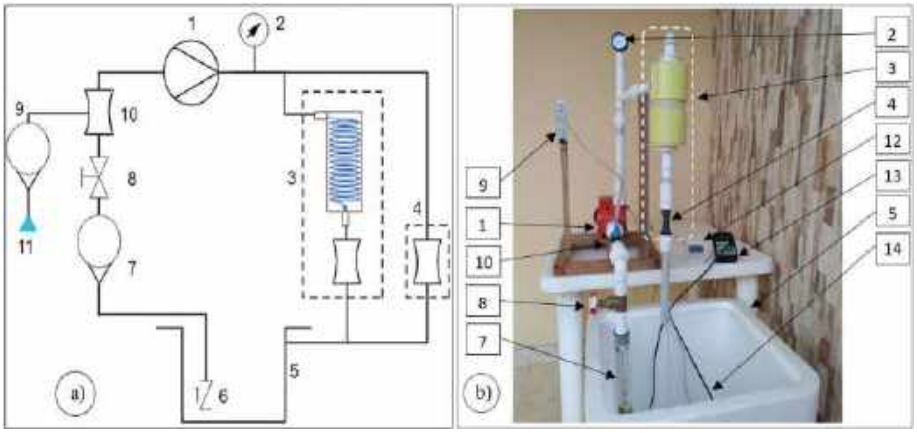

Figure 3. Experimental platform of the microbubble aeration system. (a) Experimental scheme; (b) Experimental platform with the Venturi-Vortex generator. 1-Hydraulic pump (1/2 hp); 2-Pressure gauge; 3-Venturi-Vortex generator; 4-Venturi generator; 5-Storage tank; 6-Retention valve; 7-Water Rotameter; 8-Gate valve; 9-Air rotameter; 10-Venturi for water-air mixture; 11-Atmospheric air intake; 12-Wattmeter; 13-Polarographic probe oximeter, 14-Movable wall plate.

It can be seen that element 10 of Figure 3 has the Venturi tube as is described in previous section, to supply water and air without an air compressor. The MBG can be seen on the discharge side of the pump, indicated as devices 3 and 4. The operating mode of these Venturi and Venturi-Vortex generators is carried out individually as shown in Figure 3 (a). When the Venturi generator is in operation (element 4), the Venturi-Vortex generator (element 3) is turned off, and vice versa. Figure 3 (b) shows the operating mode when the Venturi-Vortex generator is ready to operate. The accuracy of the water and air flow meters is 4% and the oximeter is 2%. The resolution of the instruments is 10 mL/min, 0.2 L/min, and 0.1 mg/L for the air flowmeter, water flowmeter, and oximeter, respectively.

2.4. Experimental factors and response variables

The following factors can affect the oxygen transfer process and were selected in this study to evaluate the performance of the devices: the water-air flow ratio (FR), the water renewal time (RT), the area-volume ratio (AVR) of the water subjected to aeration and the microbubble generator (MBG). FR represents the water and air flow ratio. RT is the renewal time of the water subjected to aeration, and the AVR is the ratio between the upper area of the water tank (i.e. upper section of the tank where the water is in contact with atmospheric air) and the volume of the water tank. Likewise, AVR represents the reciprocal of the water height subjected to aeration, which provides greater flotation time for the microbubbles to maximize the transfer of oxygen. The Microbubble Generator (MBG) factor represents the comparison of the two alternatives of Venturi and Venturi-Vortex microbubble generators selected in section 2.1.

Eqs. (1), (2), and (3) are used to determine the levels of the factors water-air flow ratio (FR), renewal time (RT) and area-volume ratio of water (AVR).

$$\boldsymbol{FR} = \frac{\dot{\boldsymbol{V}}_{H_2O}}{\dot{\boldsymbol{V}}_{Air}} \tag{1}$$

$$\boldsymbol{RT} = \frac{\boldsymbol{V}}{\dot{\boldsymbol{V}}_{H_2O}} \tag{2}$$

$$\boldsymbol{AVR} = \frac{\boldsymbol{A}}{\boldsymbol{V}} \tag{3}$$

where $\dot{V}_{H_2O}$ is the water flow (L/min), $\dot{V}_{Air}$ is the air flow (mL/min), A is the upper area of the water (cm^2) and the volume of water (L).

The response variables are the standard volumetric mass transfer coefficient (K_La_{20}), the standard oxygen transfer rate (SOTR), and the standard aeration efficiency (SAE). K_La_{20} is an indicator of the rate of oxygen dissolution in water, SOTR is the amount of oxygen dissolved to water per hour in standard conditions (gO_2/h), and SAE is the standard oxygen transfer rate divided by the power requirement (gO_2/kWh) [17]. The methodology to obtain the response variables is shown below and is based on the standard "Measurement of Oxygen Transfer in Clean Water" [17]. Eq. (4) corresponds to the oxygen transfer model, Eq. (5) is obtained from Eq. (4), which corresponds to the estimation of logarithmic deficit parameters and allows determining the volumetric mass transfer coefficient (K_La). The mass transfer coefficients K_La are obtained experimentally by the logarithm of the dissolved oxygen deficit (C_S–C) every 0.5 min, where the slope is K_La.

$$\frac{dC}{dt} = K_L a(C_s - C) \tag{4}$$

$$\boldsymbol{Ln}(\boldsymbol{C_s} - \boldsymbol{C}) = \boldsymbol{Ln}(\boldsymbol{C_s} - \boldsymbol{C_o}) - \boldsymbol{K_L a}(\boldsymbol{t} - \boldsymbol{t_o}) \tag{5}$$

where dC/dt is the gas transfer rate to or from a liquid (mg/L per h), C_O is the initial DO concentration for each measurement (mg/L), t_0 and t are the initial and end times of the measurement. From K_La, the standard volumetric mass transfer coefficient (K_La_{20}) is determined using Eq. (6). Then, the SORT and SAE are obtained from Eqs. (7) and (8), respectively.

$$\boldsymbol{K_L a_{20}} = \boldsymbol{K_L a} \cdot \boldsymbol{\theta}^{(20-T)} \tag{6}$$

$$\boldsymbol{SOTR} = \boldsymbol{K_L a_{20}} \cdot \boldsymbol{C_{s20}} \cdot \boldsymbol{V} \tag{7}$$

$$\boldsymbol{SAE} = \frac{\boldsymbol{SOTR}}{\boldsymbol{P_{in}}} \tag{8}$$

According to the ASCE standard, the term θ is a constant value equal to 1.024 [17], C_{s20} is the saturated dissolved oxygen concentration at 20 °C (mg/L), T is the temperature of the water (°C) and P_{in} is the power required by the aeration system (kW). The values obtained from K_La_{20}, SOTR and SAE are normalized data in the base of water temperature at 20 °C and a barometric pressure of 1 atm.

2.5. Screening design and operating limits

In order to evaluate the influence of factors on the responses selected and to reduce the experimental cost a design of experiments is required. A 2^{k-p} factorial design was carried out using a half fraction of the design (P = 1), with a design generator D = + ABC and four central points. The analysis of the aeration process requires the use of different levels of operation for each of the four experimental factors considered, the levels

Table 1. Levels of experimental factors and characteristics of the half-fraction factorial design [18].

Factors	Units	Levels		
		Low (-)	Medium (0)	High (+)
A: Flow ratio	L/min H_2O/ L/min Air	124.0	165.3	206.7
B: renewal time	min	2.4	3.6	4.8
C: Area-volume ratio	m^2/m^3	2.3	3.5	4.6
D: Microbubble generator	-	Venturi	-	Venturi-Vortex
Factors			4	
Fraction			1/2	
Resolution			IV	
Layout generator			D = +ABC	
Definition ratio			I = ABCD	
Aliases or confused effects				
A = BCD; B = ACD; C = ABD; D = ABC; AB = CD; AC = BD; AD = BC				

of the factors are defined according to the operational limits of the experimental platform.

Due to the scale of the aeration system, the maximum air flow allowed under stationary conditions is 50 mL/min. The flow ratio, renewal time and area-volume ratio factors depend on the volume of water subjected to aeration. To guarantee the independence of the factors, the water flow rate was set at 6.2 L/min, a mobile glass plate was used to vary the area-volume ratio of the water, locating the plate in different positions. Three levels of water volume were used in the storage tank, 15, 22.5 and 30 L, respectively. Positions of the glass plate in the storage tank are shown in Annex 2. The plate could be located in different positions within the tank to vary and combine the factor levels. In this way, the independence of the factors would be achieved in all the experimental runs. The upper section of the tank has a square shape with 37.5 cm side.

The classification of positions (i), (ii), (iii), (iv) and (v) of Annex 2, have values of volume and upper area of the water that satisfy the levels of the factors in each experimental run. The factors and their levels are shown in Table 1. In each experimental run, the DO levels of the test water were reduced below 0.5 ppm, by adding reagent grade sodium sulfite (Na_2SO_3) and cobalt sulfate ($CoSO_4$) considering the recommendations of the ASCE standard.

The 2^{k-p} factorial design requires the combination of the levels of the chosen factors, this synergy produces first, second, third and fourth order effects. The denotation of first-order effects is written separately as A, B, C, and D. Second-order effects are written as AB, AC, AD, CD, BC, and BD. Likewise with third-order effects. In this work, a 2^{k-p} factorial design was used, with $k = 4$ factors and a half fraction ($p = 1$), therefore, in this type of factorial designs, effects of equal magnitude called confounding effects are obtained, which were described in Table 1. In the variance analysis, the data treatment is performed with one of the confounding effects, since the pairs of confounding effects are equivalent [18].

2.6. Data gathering

In order to establish the levels of the experimental factors, the operating conditions of water flow, air flow, amount of water and the position of the mobile wall plate were fixed for each experimental run. In the screening process, a type I error of 5% is assumed, which allows to consider a margin of error with a 95% confidence interval in the statistical analysis. This margin of 5% represents an error associated with the statistical analysis and it is important in the variance analysis, which allows identifying the statistically significant effects of the aeration process whose P value are less than 0.05. In this way, significant and non-significant variables can be detected with a 95% confidence interval in the 2^{k-p} factorial design.

Before starting data collection, it was necessary to run the aeration system for at least 40 min, to reach the operating temperature under stationary conditions. The chemicals for deoxygenation of the water were dissolved. The aeration system is started up once the DO levels reach a value lower than 0.5 ppm. With the presence of microbubbles in water, the oximeter shows the increase in DO and the data were recorded with a video camera, until obtaining a DO concentration between 90% and 95% saturation, as is established by the standard. For each experimental run, an aeration curve was obtained with DO data between 20% and 90%, in order to estimate the response variables using the procedure described in section 2.4. According to the average water temperature during the test, the volumetric mass transfer coefficient (K_La) was standardized to 20 °C. The tests were carried out in a region with a normal atmospheric pressure of 1 atm c.a.

The operating pressure in the discharge line of the aeration system was approximately 1.4 bar for all experimental runs. According to the ASCE standard, the water could be reused as long as the total dissolved solids are not greater than 2000 ppm. This is important since the deoxygenation process with sodium sulfite and cobalt chloride produces sodium sulfate. This component remains dissolved in the water and its concentration increases every time the water is reused for new experimental tests. These solids do not affect the oxygen transferred with the aeration system according to ASCE standard. The initial DO concentration of the water is a key factor in the amount of sodium sulfite and cobalt sulfate. The DO saturation concentration was estimated according to the average water temperature of each experimental run, in order to estimate the DO saturation percentage during the aeration test, and select the instantaneous DO data between 20 and 90% for the estimation of the K_La and K_La_{20}. The minimum and maximum temperature changes obtained in the experimentation were 1.3 and 4.1 °C, respectively. With the K_La_{20} determination, the SOTR and SAE were calculated.

As an example, Figure 4 (a) shows the gradual increase in DO levels for the third experimental run, Figure 4 (b) shows for the same test, the logarithmic deficit of dissolved oxygen, which approximates a linear regression model, whose slope is proportional to the volumetric mass transfer coefficient (K_La).

Figure 4 shows that increasing the DO of water decreases the logarithmic deficit of DO. The KLa, the electrical consumption of the hydraulic pump and the values of the response variables K_La_{20}, SOTR and SAE, are shown in Table 2 for each run.

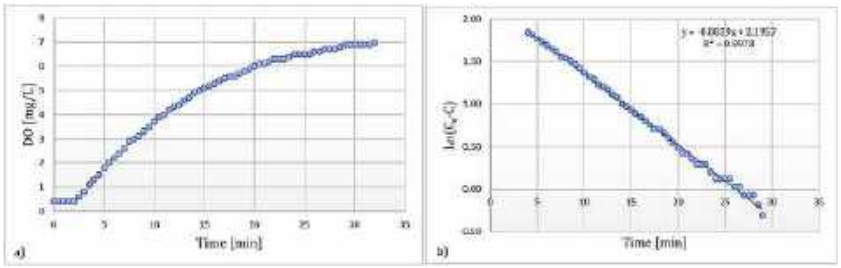

Figure 4. Aeration curves. (a) Increase in dissolved oxygen; (b) logarithmic dissolved oxygen deficit.

Table 2. Experimental factors and response variables.

Run	Non-standard parameters		Experimental factors				Response variables		
	K_La [h^{-1}]	Average electrical power consumed [W]	Flow ratio	Renewal time [min]	Area/volume ratio [m2/m3]	MB generator	K_La_{20} [h^{-1}]	SOTR [g O_2/h]	SAE [g O_2/kWh]
1	5.9	288	124.0	4.8	4.6	Venturi	4.6	1.3	4.4
2	9.3	268	124.0	2.4	2.3	Venturi	7.3	1.0	3.7
3	5.0	280	165.3	3.6	3.5	Venturi	4.0	0.8	2.9
4	8.8	271	206.7	2.4	2.3	Venturi-Vortex	7.1	1.0	3.5
5	5.4	265	124.0	4.8	2.3	Venturi-Vortex	4.4	1.2	4.5
6	7.0	267	206.7	2.4	4.6	Venturi	5.6	0.8	2.9
7	7.6	273	165.3	3.6	3.5	Venturi-Vortex	6.2	1.3	4.6
8	10.5	269	165.3	3.6	3.5	Venturi-Vortex	8.5	1.7	6.5
9	5.0	266	206.7	4.8	2.3	Venturi	4.0	1.1	4.1
10	3.7	284	206.7	4.8	4.6	Venturi-Vortex	3.0	0.8	2.8
11	2.9	275	165.3	3.6	3.5	Venturi	2.3	0.5	1.7
12	14.3	273	124.0	2.4	4.6	Venturi-Vortex	11.5	1.6	5.7

3. Statistical analysis

The screening design evaluate the impact of the experimentation factors, to identify the statistically significant variables of the aeration process. The Bartlett, Shapiro-Wilk and Durbin-Watson statistical tests were used to verify the assumption of homoscedasticity, normality and independence, respectively.

3.1. Analysis of variance

Table 3 shows the analysis of variance as a function of the response variables, K_La_{20}, SOTR and SAE. Annex 3 shows the Pareto chart of the standardized effects. According to Annex 3 (a) it is observed that the RT is a statistically significant factor with respect to the standard volumetric mass transfer coefficient (K_La_{20}). In addition, the Annex 3 (b) and (c) show that the MBG and FR factors represent the effects of greater magnitude compared to the AVR.

3.3. Verification of homoscedasticity, normality and independence of the residuals

Table 4 shows the analytical test of Bartlett, Shapiro-Wilk and Durbin-Watson, with P values greater than 0.05, which allows the verification of compliance with the assumptions of homoscedasticity, normality and independence of the residuals.

4. Results and discussion

The screening experimentation process identifies the significant and non-significant variables of the MB aeration process in clean water. It was possible to determine that the factor "water renewal time" is a statistically significant variable of the standard volumetric transfer coefficient (K_La_{20}).

By excluding the second-order effects of the model obtained in the screening process, the pure effects are graphically analyzed concerning to K_La_{20}. Figure 5 shows the response surfaces for K_La_{20} comparing the different factors analyzed. As is shown in Figure 5 (b), high values of the standard volumetric mass transfer coefficient (K_La_{20}) are obtained when the renewal time is minimal, i.e. less volume of water used or a higher water flow rate. For a longer renewal time, the value of the K_La_{20} decreases. This is consistent because oxygen diffusion is faster using a lower amount of water or a higher flow rate of MB water. In addition, by recirculating the water with a higher concentration of dissolved oxygen, the discharge flow is mixed with a proportion of MB, generated by the Venturi or Venturi-Vortex device, and this allows the concentration of DO in the water to be gradually increased each time that the fluid is recirculated.

Table 3. Analysis of variance.

Response variable	Statistical parameters	Variation source								
		A	B	C	D	AB	AC	BC	Total error	Total (corr.)
K_La_{20}	Sum of squares	8.3253	29.7953	0.4896	13.5129	2.0331	6.0778	1.5234	11.8079	73.5654
	Degrees of freedom	1	1	1	1	1	1	1	4	11
	Mean square	8.3253	29.7953	0.4896	13.5129	2.0331	6.0778	1.5234	2.9520	-
	Statistical Fo	2.8202	10.0933	0.1658	4.5776	0.6887	2.0589	0.5161	-	-
	P value	0.1684	0.0336	0.7047	0.0991	0.4533	0.2246	0.5123	-	-
SOTR	Sum of squares	0.2436	0.0006	0.0035	0.3781	0.0090	0.1607	0.0421	0.5578	1.3954
	Degrees of freedom	1	1	1	1	1	1	1	4	11
	Mean square	0.2436	0.0006	0.0035	0.3781	0.0090	0.1607	0.0421	0.1394	-
	Statistical Fo	1.7469	0.0044	0.0253	2.7112	0.0644	1.1527	0.3015	-	-
	P value	0.2568	0.9503	0.8813	0.1750	0.8122	0.3434	0.6121	-	-
SAE	Sum of squares	3.1300	0.0000	0.0000	5.3801	0.1458	1.9110	0.9140	7.9097	19.3906
	Degrees of freedom	1	1	1	1	1	1	1	4	11
	Mean square	3.1300	0.0000	0.0000	5.3801	0.1458	1.9110	0.9140	1.9774	-
	Statistical Fo	1.5829	0.0000	0.0000	2.7208	0.0737	0.9664	0.4622	-	-
	P value	0.2768	0.9989	0.9992	0.1744	0.7994	0.3812	0.5339	-	-

Table 4. Verification of the assumptions of homoscedasticity, normality and independence.

Response variable	Bartlett's test			Shapiro-Wilk test		Durbin-Watson test	
	Factor	Statistical χ_o^2	P-value	Statistical W	P-value	Statistical	P-value
K_La_{20}	A	3.899	0.142	0.903	0.171	1.735	0.274
	B	3.899	0.142				
	C	3.899	0.142				
	D	0.628	0.428				
SOTR	A	3.366	0.186	0.910	0.213	1.300	0.068
	B	3.366	0.186				
	C	3.366	0.186				
	D	0.032	0.857				
SAE	A	3.365	0.186	0.905	0.182	1.329	0.077
	B	3.365	0.186				
	C	3.365	0.186				
	D	0.058	0.809				

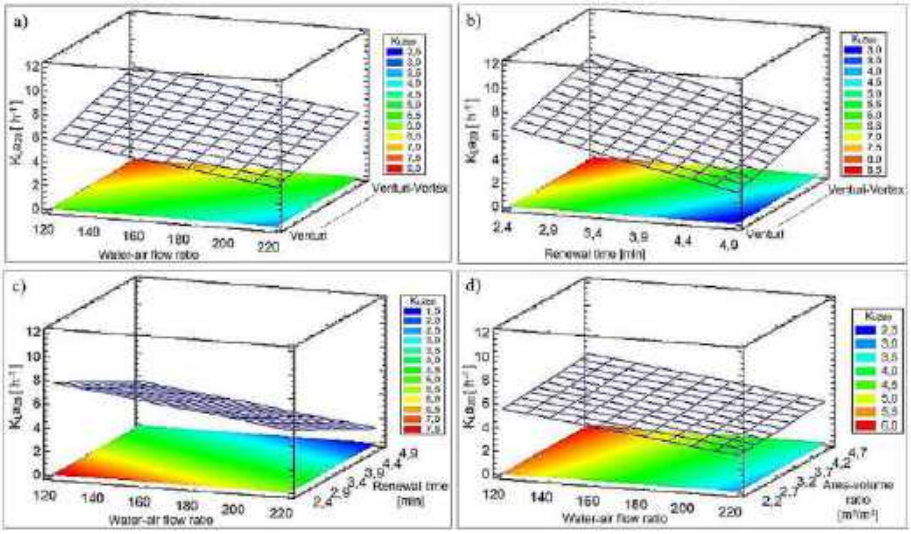

Figure 5. Response surfaces for K_La_{20}. (a) K_La_{20} with flow ratio - Type of generator; (b) K_La_{20} with renewal time - Generator type; (c) K_La_{20} with flow ratio - renewal time; (d) K_La_{20} with flow ratio vs area-volume ratio.

In Figure 5, a tendency to increase the K_La_{20} coefficient is observed when the Venturi-Vortex generator is used and the flow ratio decreases. In the case of Figure 5 (d) a substantial increase in K_La_{20} concerning the AVR is not observed. The AVR is the reciprocal of the water column, this could indicate that the variation of the water height does not produce a significant change in mass transfer due to the ability of the microbubbles to spread throughout the water.

Maximizing the K_La_{20} does not mean optimizing the aeration process, because the K_La_{20} is maximum for a minimum volume of water or when the water flow rate is increased. Optimization of the aeration process can be achieved with an acceptable and permanent dissolved oxygen level for a higher volume of water. Therefore, it is necessary to analyze the results obtained with the SOTR and SAE.

Figure 6 shows the trend of SOTR and SAE respecting to the experimental factors. When analyzing the trends of the graphs in this figure, it is found that the factors with the greatest influence on the response variables of SOTR and SAE are the MBG and the flow ratio. Figure 6 (c) and (d) show that the renewal time and the area-volume ratio factors have a smaller effect on SOTR and SAE. Figure 6 (a), (c) and (d), show that as the water-air flow ratio decreases, the oxygen transfer rate and aeration efficiency increase. Decreasing the flow ratio implies increasing the air flow in the aeration system. For this reason, MB aeration systems must be designed in such a way that admits a large flow of air. In the case of Figure 6 (a) and (b), it is observed that the use of the Venturi-Vortex device allows obtaining a positive variation in the SOTR and SAE.

The SAE trend shows the same pattern described in Figure 6. The optimal configuration of the experimental factors based on the K_La_{20}, SOTR and SAE can be achieved using a low level of FR, a low level of RT, a high level of AVR and the use of the Venturi-Vortex generator.

5. Conclusions

In this work, two options of MBG for aeration were proposed and experimentally analyzed. Performance in energy and aeration terms was evaluated using K_La_{20}, SOTR and SAE indicators. In the proposed aeration system, the air injection was made from the suction side of a pump. With this feature, a greater generation of microbubbles was obtained compared to the air injection in the throat of the Venturi generator located on the pump discharge side.

The K_La_{20} coefficient, SOTR and SAE, were evaluated as a function of the water-air flow ratio, water renewal time and area-volume ratio for both microbubble generators Venturi and Venturi-Vortex. The analysis for the K_La_{20} indicates that the input variable renewal time is a statistically significant factor of the aeration process, K_La_{20} can be

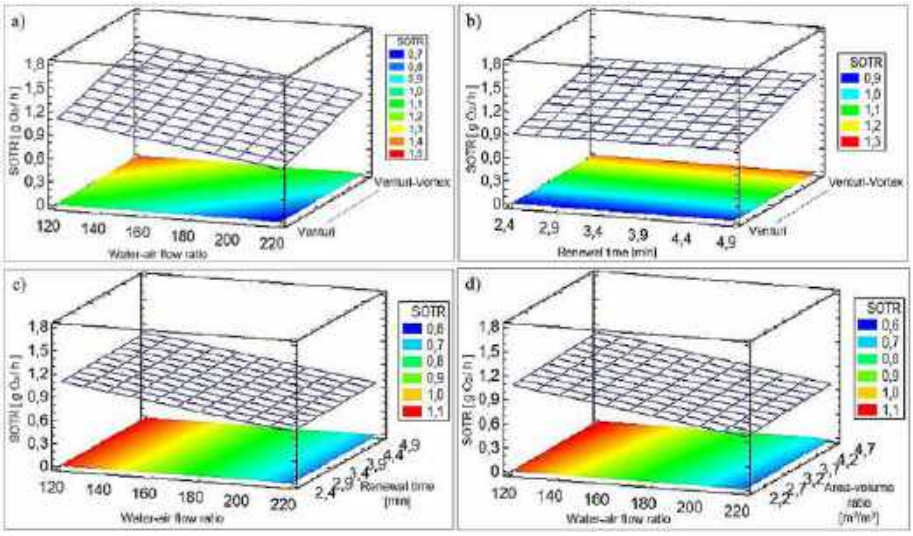

Figure 6. Response surface for SOTR.

maximized using a minimum RT. To minimize the RT, water flow in the system could be increased or the volume of water decreased. Considering a commercial application, it is more convenient to increase the water flow.

Results allows to conclude that the Venturi-Vortex MBG has the best performance, using a minimum flow ratio. The trends show that with the use of the Venturi-Vortex generator instead of the individual Venturi generator, a higher value of K_La_{20}, SOTR and SAE is obtained. From a qualitative observation, it seems that the Venturi-Vortex generator offers a better performance due to its ability to generate microbubbles, which provide a larger contact area with the water to increase oxygen transfer. In addition, the injection of air on the suction side of the hydraulic pump allows the generation of a greater number of microbubbles, using a low level of RF, that is, providing a greater flow of air in the system.

More research is required in designs of aeration systems that allow a high conversion of large bubbles to microbubbles, using devices that promote a combined effect of vorticity and sudden deceleration as that produced in the divergent zone of a Venturi generator.

Declarations

Author contribution statement

Esteban De Oro Ochoa, Mauricio Carmona García, Néstor Durango Padilla, Andrés Martínez Remolina: Conceived and designed the experiments; Performed the experiments; Analyzed and interpreted the data; Contributed reagents, materials, analysis tools or data; Wrote the paper.

Funding statement

This research did not receive any specific grant from funding agencies in the public, commercial, or not-for-profit sectors.

Data availability statement

Data included in article/supp. material/referenced in article.

Declaration of interests statement

The authors declare no conflict of interest.

Acknowledgements

The authors thank the Ministry of Science, Technology and Innovation of Colombia for the support provided within the framework of the "Formación de Capital Humano de Alto Nivel Para las Regiones: La Guajira" program.

Additional information

Supplementary content related to this article has been published online at http://doi.org/10.1016/j.heliyon.2022.e10824.

References

[1] A. Kumar, S. Moulick, B.C. Mal, Selection of aerators for intensive aquacultural pond, Aquac. Eng. 56 (2013) 71–78.
[2] B.C. Mal, Chapter 3-Aeration system for aquaculture, Aquac. Facil. Equip. (2021) 67–123.
[3] N. Suwartha, D. Syamzida, C.R. Priadi, S.S. Moersidik, F. Ali, Effect of size variation on microbubble mass transfer coefficient in flotation and aeration processes, Heliyon 6 (4) (2020), e03748.
[4] J. Huang, L. Sun, H. Liu, Z. Mo, J. Tang, G. Xie, M. Du, A review on bubble generation and transportation in Venturi-type bubble generators, Exp. Comput. Multiph. Flow 2 (3) (2020) 123–134.
[5] A. Yadav, A. Kumar, S. Sarkar, Performance evaluation of venturi aeration system, Aquac. Eng. 93 (March) (2021), 102156.
[6] L. Zhao, Z. Mo, L. Sun, G. Xie, H. Liu, M. Du, J. Tang, A visualized study of the motion of individual bubbles in a venturi- type bubble generator, Prog. Nucl. Energy 97 (2017) 74–89.
[7] C.H. Lee, H. Choi, D.W. Jerng, D.E. Kim, S. Wongwises, H.S. Ahn, Experimental investigation of microbubble generation in the venturi nozzle, Int. J. Heat Mass Transf. 136 (2019) 1127–1138.
[8] M. Li, A. Bussonnière, M. Bronson, Z. Xu, Q. Liu, Study of Venturi tube geometry on the hydrodynamic cavitation for the generation of microbubbles, Miner. Eng. 132 (April 2018) (2019) 268–274.
[9] X. Yu, P. Felicia, Optimization of cavitation venturi tube design for pico and nano bubbles generation, Min. Sci. Technol. (2015) 1–7.
[10] E.D. Michailidi, G. Bomis, A. Varoutoglou, G.Z. Kyzas, G. Mitrikas, A. Ch, Mitropoulos, E.K. Efthimiadou, E.P. Favvas, Bulk nanobubbles: production and investigation of their formation/stability mechanism, J. Colloid Interface Sci. 564 (2020) 371–380.
[11] X. Wang, Y. Shuai, H. Zhang, J. Sun, Y. Yang, Bubble breakup in a swirl-venturi microbubble generator, Chem. Eng. J. 403 (July 2020) (2021), 126397.
[12] X. Wang, Y. Shuai, X. Zhou, Z. Huang, Y. Yang, J. Sun, H. Zhang, J. Wang, Y. Yang, Performance comparison of swirl-venturi bubble generator and conventional venturi bubble generator, Chem. Eng. Process. Process Intensif. 154 (March) (2020), 108022.
[13] A. Agarwal, W.J. Ng, Y. Liu, Principle and applications of microbubble and nanobubble technology for water treatment, Chemosphere 84 (9) (2011) 1175–1180.

[14] M.S. Kim, M. Han, T. Il Kim, J.W. Lee, D.H. Kwak, Effect of nanobubbles for improvement of water quality in freshwater: flotation model simulation, Sep. Purif. Technol. 241 (December 2019) (2020).
[15] E.P. Favvas, G.Z. Kyzas, E.K. Efthimiadou, A.C. Mitropoulos, Bulk nanobubbles, generation methods and potential applications, Colloid Interface Sci. 54 (2021), 101455.
[16] J.Y. Kim, M.G. Song, J.D. Kim, Zeta potential of nanobubbles generated by ultrasonication in aqueous alkyl polyglycoside solutions, J. Colloid Interface Sci. 223 (2) (2000) 285–291.
[17] American Society of Civil Engineers (ASCE), Measurement of Oxygen Transfer in Clean Water, American National standards Institute (ANSI), 1852.
[18] D.C. Montgomery, Design and Analysis of Experiments vol. 9, Limusa Wiley, 2017.